

Preparation of nano-scale Cr_3C_2 particles dispersed on alumina particles by MOCVD in fluidized reactor and carbothermal treatment

Hao-Tung Lin^a, Jow-Lay Huang^{a,*}, Sheng-Chang Wang^b, Chen-Fu Lin^a

^a Department of Materials Science and Engineering, National Cheng-Kung University, Tainan 701, Taiwan, ROC

^b Department of Mechanical Engineering, Southern Taiwan University of Technology, Tainan 710, Taiwan, ROC

Received 25 March 2005; accepted 29 July 2005

Available online 9 November 2005

Abstract

Nano-scale Cr_3C_2 powder with an average particle size of 50–80 nm, uniformly coated on alumina particles, has been prepared by metal organic chemical vapor deposition (MOCVD) in the fluidized chamber, using the pyrolysis of $\text{Cr}(\text{CO})_6$ precursor, and carbothermal treatment in the CH_4 and H_2 gas mixtures. The $\text{Cr}(\text{CO})_6$ precursor was characterized by differential scanning calorimetry (DSC) to understand the decomposition temperature of the precursor, which was determined to be 163 °C. The precursor decomposed and formed the mixture of CrC_{1-x} , Cr_2O_3 and free carbon on the surface of the Al_2O_3 particles when pyrolyzed in fluidized bed at 300 and 400 °C. The resultant powders were examined by X-ray diffractometer (XRD) and transmission electron microscopy (TEM) equipped with energy dispersion spectrometer (EDS), for investigating phase composition and microstructures. The as-deposited particles fabricated at 300 and 400 °C in fluidized chamber were amorphous and crystalline, respectively. The thermal behaviour investigated by TG/DTA indicates that the amorphous powder had a exothermic peak in the DTA curve at ~400 °C, which crystallized at this temperature. In order to prepare the nano-particle reinforced composites, the powder fabricated in the fluidized bed was carbonized in the mixed atmosphere of CH_4 and H_2 . Both CrC_{1-x} and Cr_2O_3 phase were transferred into Cr_3C_2 phase after the carbothermal treatment.

© 2005 Elsevier B.V. All rights reserved.

Keywords: Nano-scale; Pyrolysis; Metal organic chemical vapor deposition (MOCVD); Chromium carbide

1. Introduction

Alumina has been broadly used because it possesses excellent mechanical properties, and good chemical stability. However, because of covalent bonding, it has inherently low fracture toughness and plastic deformation, which limited the application. Therefore, to improve the toughening of alumina ceramics is an important and challenging area. Incorporation of secondary phases (e.g. particulates, fibers, or platelets) has been proven to be an easy, safe and economical toughening technique for alumina ceramics [1–3]. Among the reported toughening methods [4–7], the incorporation of hard particulate reinforcement is the best effective technique for toughening of alumina ceramics. Chromium carbide (Cr_3C_2) successfully incorporated into Al_2O_3 for toughening purposes owing to its properties such as high hardness, high melting point, high Young's modulus

and high temperature erosion resistance [4]. Quite promising mechanical properties and high temperature oxidation resistance of chromium carbide/alumina composites were reported in the literatures [4,8–10].

Niihara reported the advantages of nano-meter inclusions could achieve several benefits [11], such as the reduction of grain size of matrix grains, strengthening and toughening. For preparing particle-reinforced composite, nano-scale reinforcing particles are difficult to uniformly disperse on the micro-scale matrix particles by using traditional mixing technique. This problem is ascribed to that the nano-sized particles are easy to agglomerate due to the high attractive force energy between the particles [12]. The agglomerate will promote the generation of voids during the densification and microstructural non-homogeneity [13].

There are many advantages for preparing nano-composite in a fluidized bed reactor. An even temperature can be achieved because the alumina particles are in constant motion in the reaction vessel and the large common area of the gas and solid particles ensures that the heat transfer rate is fast. Therefore, the fluidized bed reactor could supply an environment with uniform

* Corresponding author. Tel.: +886 6 234 8188; fax: +886 6 276 3586.
E-mail address: JLH888@mail.ncku.edu.tw (J.-L. Huang).

temperature and concentration of the coating precursor that can provide the possibility of good dispersion of the nano-particles on the matrices [14].

It has been found that the combination of conventional fluidized bed technology with chemical vapor deposition (CVD) is an effective method to deposited particles. Morooka et al. [15] fluidized fine Al_2O_3 particles and coated them uniformly with TiO_2 crystallites formed by the oxidation of TiCl_4 and TiN particles were deposited on the surface of fluidized Si_3N_4 particles. Tsugeki et al. [16] introduced Al_2O_3 crystallites were coated with TiN crystallites formed by the reaction of TiCl_4 with NH_3 in a fluidized bed reactor. Wood et al. [17] coated the aluminum, titanium, and titanium nitride on mica, and alumina on nickel. Hua and Li [18] reported the nano-crystalline SnO_2 films on Al_2O_3 particles. In this work, the $\text{Cr}(\text{CO})_6$ was used as a precursor, which coated on Al_2O_3 matrices by MOCVD in fluidized bed. The decomposition of the precursor $\text{Cr}(\text{CO})_6$, and the as-deposited particles were analyzed. Furthermore, in order to form the reinforced nano-chromium carbide particles in the alumina matrix, carbothermal treatment was performed and characterizations of treated powder were discussed in this paper.

2. Experimental

Chromium hexacarbonyl ($\text{Cr}(\text{CO})_6$, 99%, Strem Chemicals Co., USA) was used as precursor of chromium oxide in the MOCVD process. Aluminum oxide powder (A16SG, Alcoa, USA) was used as matrix powder, the average size was about 0.7 μm . The vapor of precursor was carried by He gas (99.9% pure) that was introduced into the fluidized bed reactor for MOCVD process. Based on Lander's and Germer's results [19], the precursor container was kept at 75 °C in vacuum (10 Torr) in present experiment. $\text{Cr}(\text{CO})_6$ vapor was decomposed in the fluidized chamber, at 300 and 400 °C, respectively, and it would deposit on the fluidizing alumina particles in the chamber. A detail description of the process was shown in our previous paper [20].

The precursor was characterized by DSC (differential scanning calorimetry, TA Instrument Model 2920, USA). The deposited particles were analyzed by XRD (Rigaku D/Max III, Japan), DTA (NERZSCH STA 409 PC), and TEM (Hitachi FE-2000 field Emission Transmission Electron Microscopy) equipped with energy dispersive X-ray spectroscopy (EDS) to identify the phase composition, morphology. XPS (X-ray photoelectron spectroscopy, VG Scientific 210, England) was used to characterize the coating phases by binding energy. BET instrument (Micromeritics Gemini 2360, USA) was used to measure the specific surface area by nitrogen adsorption, and C/O analyzer (LECO CS-244, USA) was used to measure the carbon content of coated powder by a combustion method. The thermal behavior of the particles prepared in fluidized bed was investigated by difference thermal analysis/thermogravimetry (DTA/TG, GravitNERZSCH STA 409 PC, Germany). The as-deposited particles were carbothermally treated in CH_4 and H_2 gas mixture.

3. Results and discussion

3.1. Analysis of $\text{Cr}(\text{CO})_6$ precursor

Fig. 1 is the DSC analysis of the $\text{Cr}(\text{CO})_6$ precursor, where the heating rate was 10 °C in the N_2 atmosphere which shows the dissociation of this metallic carbonyls began at 150 °C with an endothermic peak at 163 °C. This temperature is very close to the observed decomposition temperature reported by Lide [21]. Again, Lo and Wei [22] reported that the deposited film had better mechanical properties when the pyrolysis temperature was from 300 °C up to 400 °C. And Chen and Wei [23] indicated that

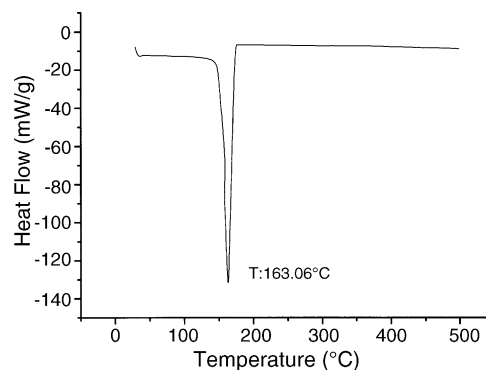


Fig. 1. Differential scanning calorimetry (DSC) curve of the precursor $\text{Cr}(\text{CO})_6$.

pyrolyzed at 400 °C had higher deposition rate, therefore, in order to compare decomposition of $\text{Cr}(\text{CO})_6$ at different temperature, the carbonyl gas molecules were vaporized as gas stream, which flowed into the fluidized chamber with temperature 300 and 400 °C.

Firstly, in this study, only the precursor was heated and alumina powder was not added as matrix in the fluidized bed, the powder attached on the chamber wall was collected to do analysis. The TEM micrograph of the as-deposited particles prepared at 300 °C for 30 min was shown in Fig. 2. It is clearly observed that the particles were in the shape of sphere with a size of about 10–40 nm. The XPS spectra of C 1s and Cr 2p regions of the as-deposited powder prepared at 300 °C are displayed in Figs. 3 and 4. The XPS spectra of the C 1s regions in Fig. 3 provide the evidence for which at least two forms of carbon exist in the as-deposited powder. One is carbon bonded to chromium atoms (C–Cr) at 283.5 eV and the other is free carbon (C–C) at 284.6 eV. Fig. 4 indicates two peaks corresponding to the spin-orbit splitting $2p_{1/2}$ and $2p_{3/2}$ of Cr, which has bonding energy of 586.3 and 576.6 eV, respectively. The band shift of these two peaks is 9.7 eV, which is consistent with previously

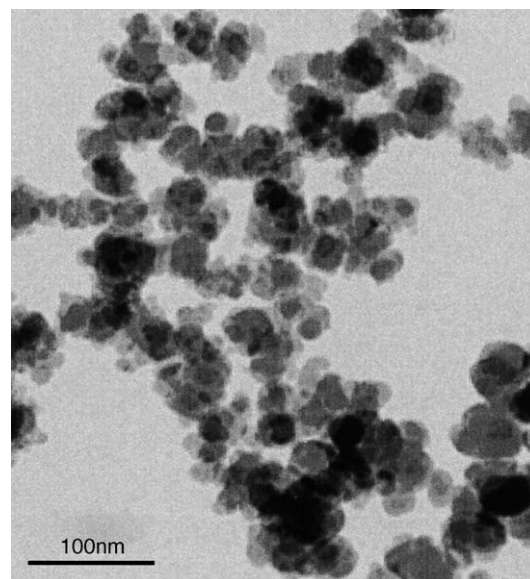


Fig. 2. TEM micrograph of nano-particles prepared at 300 °C.

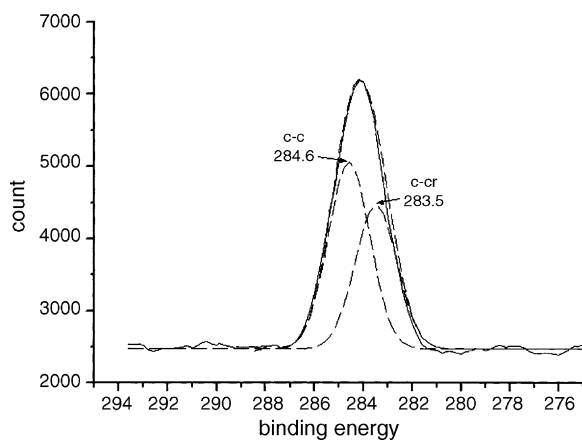


Fig. 3. X-ray photoelectron spectra of the C 1s regions of fluidized composite powder prepared at 300 °C in fluidized bed.

reported data [24], and confirms the existence of Cr_2O_3 particles in the as-deposited powder. After the pyrolysis, the CO ligands in $\text{Cr}(\text{CO})_6$ disappeared [25] and the produced species include Cr, and CO. However, Shinn and Madey [26] reported that the CO molecules were unstable and had a tendency to chemisorb onto the surface of transit metals and the bond between carbon and oxygen would break when the chemisorption occurred. The possible reaction species were Cr, Cr–C, C and O in the fluidized chamber. Therefore, XPS result shows products of as-deposited particles are Cr_2O_3 , carbide (Cr–C) and free carbon are reasonable.

Fig. 5 shows two XRD patterns of the resultant powders obtained at 300 and 400 °C. Although both testing temperatures lead to a pyrolysis effect, the Cr_2O_3 powders generated at 300 °C were found to be amorphous as indicated by Fig. 5(a), whereas the product generated at 400 °C were found to be crystalline Cr_2O_3 with hexagonal structure and CrC_{1-x} phase with NaCl (B1) structure [27], as marked in Fig. 5(b). Schuste and Maury [28] reported that the CrC_{1-x} phase and free carbon were fabricated in the coating when $\text{Cr}(\text{CO})_6$ was used as the precursor of MOCVD process. Bouzy et al. [27] proposed that non-stoichiometric CrC_{1-x} was a metastable phase, and inter-

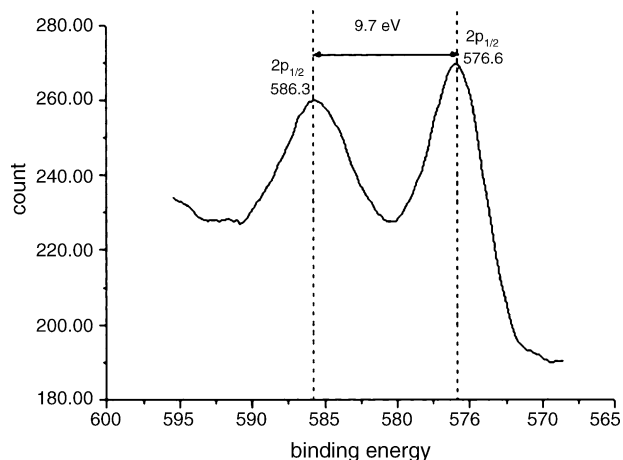


Fig. 4. X-ray photoelectron spectra of the Cr 2p regions of the fluidized composite powder prepared at 300 °C in fluidized bed.

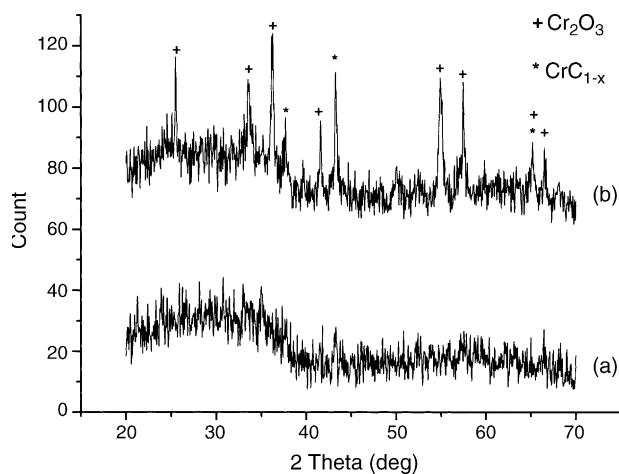


Fig. 5. XRD patterns of the fluidized powders prepared at (a) 300 °C; (b) 400 °C.

preted that small C atoms inserted in the octahedral interstitial sites of the cubic-close Cr packings in this structure. From the report of Bewilogua et al. [29], this NaCl (B1) structure was also found in Cr–C films prepared by ion-plating. The broadening of diffraction peaks and the visible fluctuated background imply that the particles were nano-scale [30] and some nano-particles were not fully crystallized.

Fig. 6 shows the TEM electron diffraction pattern of the nano-particle prepared at 300 and 400 °C. Fig. 6(a) confirmed that Cr_2O_3 synthesized at 300 °C was amorphous, and Fig. 6(b) and (c) demonstrate two types of crystalline particles in the as-deposited powder: Cr_2O_3 phase with hexagonal structure and CrC_{1-x} phase with NaCl (B1) structure, in agreement with the results of XRD shown in Fig. 5.

Fig. 7 is the TG/DTA curves of the amorphous and crystalline particles prepared at 300 and 400 °C in fluidized bed, respectively. The particles were heated from 30 to 900 °C at a heating rate of 10 °C min^{-1} in Ar atmosphere. Comparing the DTA curves of amorphous and crystalline powder, it is found that there is an exothermic peak in the curve of amorphous powder appears at ~ 400 °C, which is because of the crystallization of nano-scale amorphous particles at that temperature. The maximum of the peak is appeared at 415 °C. TG curve indicates that the mass of powder loses with the temperature increased in both amorphous and crystalline powder, owing to the volatilities of CO and CO_2 from the powder. There is a sharp mass loss around the crystalline temperature, it implies that the carbon content in the crystalline powder was obviously lower than in the amorphous.

3.2. Nano-particles deposited on the alumina after being fluidized

Fig. 8 displays the TEM micrograph of the as-deposited particles with size 20–30 nm well-dispersed on the surfaces of alumina particles when composite prepared in the fluidized chamber at 300 °C for 2 h. Table 1 shows the carbon content of the samples prepared at 300 and 400 °C was 0.75 and 0.23%, respectively. It indicates the as-deposited amorphous powder

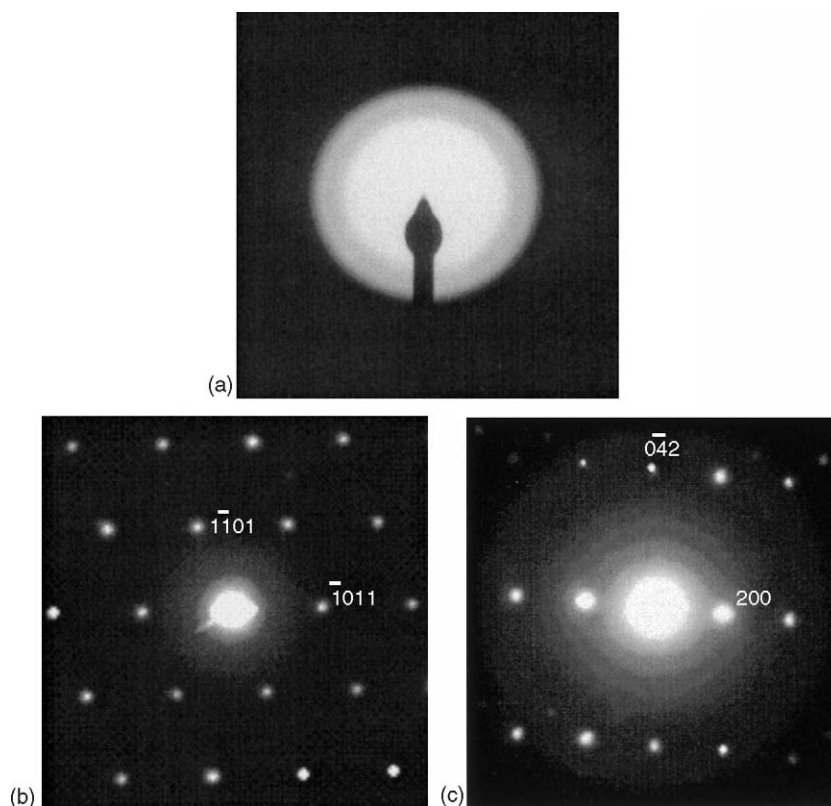


Fig. 6. TEM diffraction patterns of the coated particles (a) prepared at 300 °C in fluidized bed, showing amorphous phase; (b) and (c) prepared at 400 °C in fluidized bed. (b) Cr₂O₃ phase with hexagonal structure; and (c) CrC_{1-x} phase with NaCl (B1) structure, respectively.

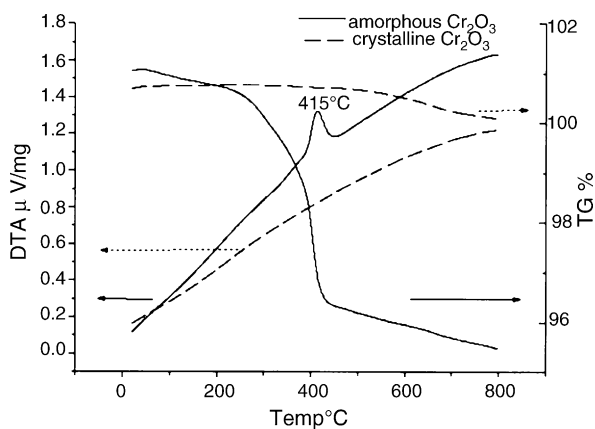


Fig. 7. The DTA curves of the amorphous and crystalline fluidized powder at a heating rate of 10 °C min⁻¹ in Ar atmosphere.

prepared at 300 °C had more carbon content than the crystalline powders prepared at 400 °C. This was probably due to the amorphous powders had larger specific surface area than crystalline powders.

Table 1
The specific surface area and carbon content of samples

	Sample 1	Sample 2
Fluidized condition	300 °C/2 h	400 °C/2 h
Carbon content (%)	0.75	0.23
BET surface area (m ² /g)	25.5	11.2

Fig. 9 shows the EDS results of the particle “A” indicated in the Fig. 8. It indicates that the particle “A” was composed of element C, Cr and O, meanwhile, the element Cu from Cu grid was also detected. From the EDS results, it proved that the particles coated on alumina were formed through the deposition of the pyrolysis of precursor.

Above result indicates that the vaporized Cr(CO)₆ precursor can be deposited on the surfaces of fluidizing alumina particles

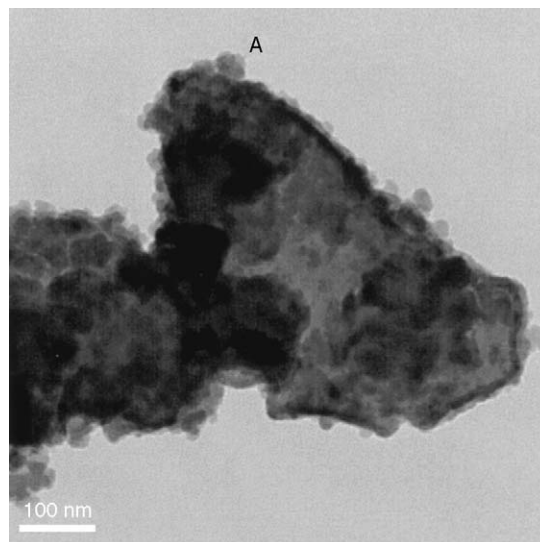


Fig. 8. TEM micrograph of nano-particles deposited on the surface of Al₂O₃ particles.

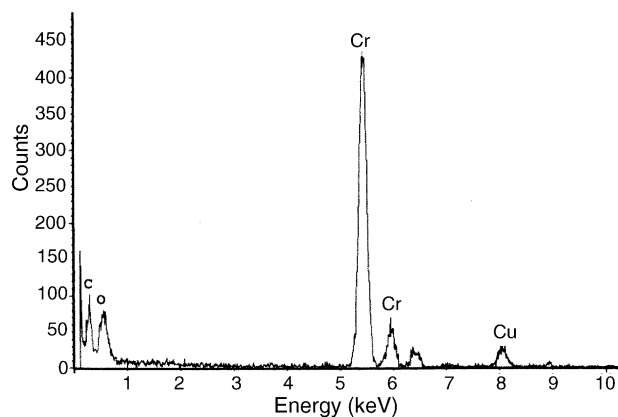
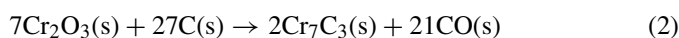


Fig. 9. EDS results of the deposited particle A of Fig. 8.

through the pyrolysis effect by mean of a combination of chemical vaporized deposition and fluidized bed technique.

3.3. Carbothermal treatment of the as-deposited powder

From previous paper [20], after the thermal treatment at 1150 °C in graphite chamber, the Cr_2O_3 particles in as-deposited powder prepared at 300 °C transferred into monolithic Cr_3C_2 phase, while the powder prepared at 400 °C transferred into mixed phases of Cr_3C_2 and Cr_7C_3 . According to the Table 1, the former had enough carbon content to form monolithic Cr_3C_2 , but the latter formed both chromium carbide, Cr_3C_2 and Cr_7C_3 , owing to the carbon content was not enough. The Eqs. (1) and (2) explain more content of carbon is needed for Cr_2O_3 to form Cr_3C_2 , otherwise the Cr_7C_3 is formed [31].



To reduce the carbothermal temperature of Cr-spices particles and prevent the pre-sintering of the Al_2O_3 particles at elevated temperature, CH_4 and H_2 gas mixture were adopted in the thermal treatment process. From the report of Loubtere et al. [32], the chromium oxide was carbonized in the CH_4 and H_2 gas mixtures and transferred into chromium carbide (Cr_3C_2). Fig. 10 displays the XRD patterns of carbonizing powder synthesized at 700 °C for 2 h in CH_4 and H_2 gas mixture for the as deposited powder of 300 and 400 °C. The XRD patterns indicate the Cr-spices in both crystalline and amorphous powders are transformed into Cr_3C_2 owing to the enough carbon was prepared in the CH_4 and H_2 mixture atmosphere. Fig. 11(a) shows the TEM micrographs of the nano-composite particles carbothermally treated at 700 °C for 2 h in the CH_4 – H_2 gas mixtures. The Fig. 11(a) displays the nano-particles were 50–80 nm in the size. The TEM diffraction pattern of the particle “B” indicated in Fig. 11(a) is showed in Fig. 11(b), the Cr_3C_2 phase with orthorhombic structure is observed. Form the results of XRD and TEM, not only the chromium oxide was carbonized to chromium carbide (Cr_3C_2), but the CrC_{1-x} was also transferred into Cr_3C_2 during the thermal treatment. This result coincided with the reports [27,29], which reported that an annealing treatment and higher

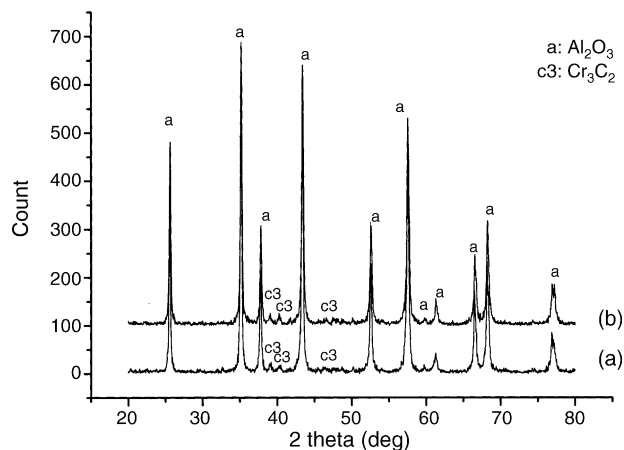


Fig. 10. XRD patterns of the carbonizing powder synthesized at 700 °C for 2 h in CH_4 – H_2 gas mixtures for the fluidized powder of (a) 300 °C; (b) 400 °C.

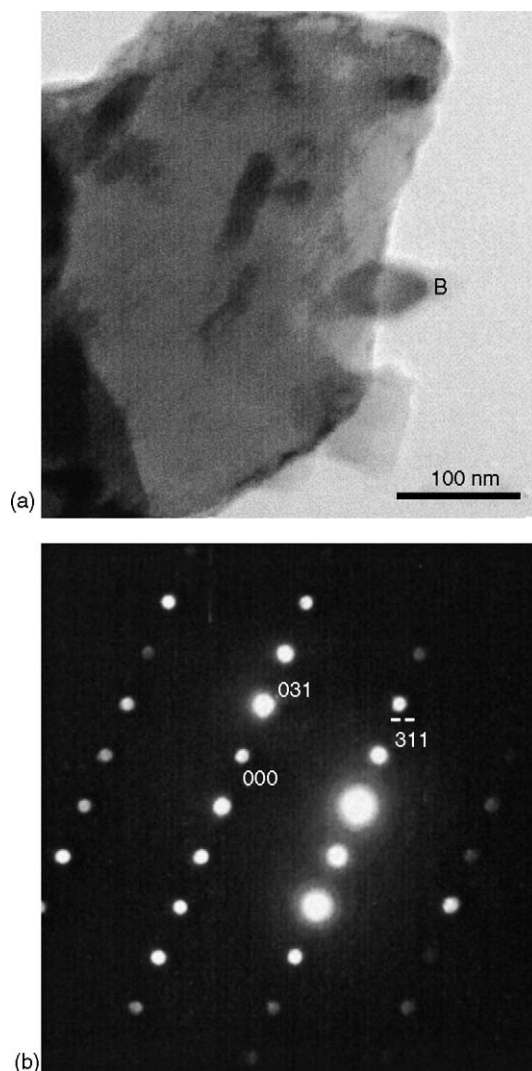


Fig. 11. (a) TEM micrographs of the nano-particles Cr_3C_2 deposited on the surface of the Al_2O_3 particles after the carbothermal treatment in the CH_4 – H_2 gas mixtures at 700 °C for 2 h; (b) TEM diffraction patterns of the particle “B” indicated in (a), showing Cr_3C_2 phase with orthorhombic structure.

content of carbon caused a transformation of the metastable carbide CrC_{1-x} into the stable carbide phase Cr_3C_2 .

4. Conclusions

Nano-scale carbide $\text{Cr}_3\text{C}_2/\text{Al}_2\text{O}_3$ composites were prepared through pyrolysis of $\text{Cr}(\text{CO})_6$ precursor by means of MOCVD combined with the fluidized technique and carbothermal treatment in the mixture of CH_4 and H_2 gas. The precursor $\text{Cr}(\text{CO})_6$ was decomposed into Cr_2O_3 , CrC_{1-x} , and free carbon, which deposited on the alumina surface in the fluidized chamber at 300 and 400 °C. The collected particles were amorphous at 300 °C pyrolysis temperature, however the crystallization of amorphous particles starts at about 400 °C, which was confirmed in the TG/DTA curve. Both the amorphous and crystalline particles of Cr_2O_3 and CrC_{1-x} fabricated at 300 and 400 °C were transformed into monolithic Cr_3C_2 phase at 700 °C in $\text{CH}_4\text{--H}_2$ gas mixtures.

Acknowledgment

The authors would like to thank National Science Council of the Republic of China for its financial support under the Contract No. NSC-92-2216-E-006-011.

References

- [1] S. Lio, M. Watanabe, M. Matsubara, Y. Matsuo, *J. Am. Ceram. Soc.* 72 (10) (1989) 1880–1884.
- [2] W.J. Tseng, P.D. Funkenbusch, *J. Am. Ceram. Soc.* 75 (5) (1992) 1171–1175.
- [3] Y.S. Chou, D.J. Green, *J. Am. Ceram. Soc.* 75 (12) (1992) 3346–3352.
- [4] C.T. Fu, J.M. Wu, A.K. Li, *J. Mater. Sci.* 29 (1994) 2671–2677.
- [5] S. Lio, M. Watanabe, M. Matsubara, Y. Matsuo, *J. Am. Ceram. Soc.* 72 (10) (1989) 1880–1884.
- [6] W.J. Tseng, P.D. Funkenbusch, *J. Am. Ceram. Soc.* 75 (5) (1992) 1171–1175.
- [7] Y.S. Chou, D.J. Green, *J. Am. Ceram. Soc.* 75 (12) (1992) 3346–3352.
- [8] C.T. Fu, A.K. Li, J.M. Wu, *J. Mater. Sci.* 28 (1993) 6285–6294.
- [9] K.M. Shu, C.T. Fu, D.M. Liu, *J. Mater. Sci. Lett.* 13 (1994) 1146–1148.
- [10] C.T. Fu, A.K. Li, J.M. Wu, *Br. Ceram. Trans.* 93 (5) (1994) 178–182.
- [11] K. Niihara, *J. Ceram. Soc. Jpn.* 99 (10) (1991) 974–982.
- [12] G.Y. Onada Jr., L.L. Hench, *Ceramic Processing before Firing*, Wiley, New York, 1978, pp. 357–376.
- [13] E.A. Pugar, P.E.D. Morgan, *J. Am. Ceram. Soc.* 69 (6) (1984) C120–C123.
- [14] D. Kumii, O. Levenspiel, *Fluidization Engineering*, Huntington, N.Y., 1977, pp. 195–223.
- [15] S. Morooka, A. Kobata, K. Kusakabe, *AIChE Symp. Ser.* 87 (1991) 32–37.
- [16] K. Tsugeki, T. Kato, Y. Koyanagi, K. Kusakabe, S. Morooka, *J. Mater. Sci.* 28 (1993) 3168–3172.
- [17] B.J. Wood, A. Sanjurjo, G.T. Tong, S.E. Swider, *Surf. Coat. Technol.* 49 (1991) 228–232.
- [18] B. Hua, C. Li, *Mater. Chem. Phys.* 59 (1999) 130–135.
- [19] J.J. Lander, L.H. Germer, *Am. Inst. Miner. Metal. Eng. Technol.* 14 (6) (1947) 1–4.
- [20] H.T. Lin, J.L. Huang, W.T. Lo, W.C.J. Wei, *J. Mater. Res.* 20 (8) (2005) 2154–2160.
- [21] D.R. Lide, *Handbook of Chemistry and Physics*, 72nd ed., CRC press, Boston, MA, 1991–92, pp. 4–76.
- [22] M.H. Lo, W.C.J. Wei, *J. Am. Ceram. Soc.* 80 (4) (1997) 886–892.
- [23] C.L. Chen, W.C. Wei, *J. Eur. Ceram. Soc.* 22 (2002) 2883–2892.
- [24] C.D. Wagner, W.M. Riggs, L.E. Davis, J.F. Moulder, *Handbook of X-ray Photoelectron Spectroscopy*, Perkin-Elmer, Minnesota, 1979, 77 pp.
- [25] A. Kazusaka, R.F. Howe, *J. Mol. Catal.* 9 (1980) 199–207.
- [26] N.D. Shinn, T.E. Madey, *J. Chem. Phys.* 83 (11) (1985) 5928–5935.
- [27] E. Bouzy, E. Bauer-Grosse, G. Le Caer, *Philos. Mag. B.* 68 (5) (1993) 619–638.
- [28] F. Schuste, F. Maury, *Surf. Coat. Technol.* 43 (1990) 185–198.
- [29] K. Bewilogua, H.-J. Heinitz, B. Rau, S. Schulze, *Thin Solid Films* 167 (1988) 233–243.
- [30] G.K. Williamson, W.H. Hall, *Acta Metall.* 1 (1953) 22–31.
- [31] W.F. Chu, A. Rahmel, *Oxid. Met.* 15 (1981) 331–337.
- [32] S. Loubtere, Ch. Laurent, J.P. Bonino, A. Rousset, *J. Alloy. Compd.* 243 (1996) 59–66.